Electronic Supplementary Material (ESI) for Green Chemistry.

Supporting Information

Blowing Tough Polylactide Film Enabled by *in Situ* Construction of Covalent Adaptive Networks with Epoxidized Soybean Oil as Dynamic Crosslinks

Yong-Bo Liu, Zhao Xu, Zheng-Min Zhang, Rui-Ying Bao,* Ming-Bo Yang, Wei Yang*

College of Polymer Science and Engineering, Sichuan University, State Key Laboratory of Polymer Materials Engineering, Chengdu, 610065, Sichuan, China

*Corresponding authors: rybao@scu.edu.cn (RY Bao) and weiyang@scu.edu.cn (W Yang)

Preparation of control group for TGA measurements. To further explore the effect of the incorporation of CANs on the thermal stability of PLA, control groups were prepared by a torque rheometer (XSS-300, Shanghai Kechuang Rubber Plastics Machinery Set Ltd, China) at 180 ˚C. Fully dried PLA was first melted at 20 rpm for 3 min, followed by the addition of 1 wt% $Zn(acac)_2$ with or without 4 wt% ESO and mixed at 60 rpm for 5 min. The obtained samples were named PLA/$Zn(acac)_2$ and PLA/$Zn(acac)_2$/ESO. PLA-g-MA/$Zn(acac)_2$ was prepared by first melting fully dried PLA-g-MA obtained by the first step extrusion at 20 rpm for 3 min, followed by adding 1 wt% Zn $(acac)_2$ and mixing at 60 rpm for 5 min. A significant increase in torque can be observed, indicating the existence of ionic dipole interaction between MA grafted to PLA and Zn^{2+}. A similar phenomenon is also observed in other polymers [1-3].

Nuclear Magnetic Resonance (NMR). The graft ratio of PLA-g-MA was determined by 400MHz ^1H NMR spectroscopy (AV III HD 400 MHz, Bruker, Switzerland) at 25 ˚C. Chloroform-d ($CDCl_3$) with TMS was used as the solvent for NMR characterization.

Fourier Transform Infrared Spectroscopy (FTIR). FTIR of ESO, neat PLA, PLA-g-MA, PLA CANs and recycled PLA CANs was performed on a Fourier transform infrared spectrometer (6700, Thermo Nicolet, USA). The scan range was 4000-500 cm^{-1}, and the number of scans was 32 times. The polarized FTIR spectroscopy was implemented by FTIR equipped with a Polaroid. A multi-angle scan from 0 to 180° was conducted by altering the polarizers′ angle. The dichroic ratio (D) and orientation function (f) were deduced using relations[4]

$$D = A_{\parallel} / A_{\perp}$$

$$f = (D - 1)/(D + 2)$$

For PLA, absorption at 956 cm^{-1} is due to the contribution of amorphous phases. The orientations of the amorphous phase (f_a) are determined by 956 cm^{-1} bands.

Creep Measurements. The creep experiments of neat PLA and PLA CANs melts were carried out at 185°C by a rheometer (AR 2000EX, TA, USA), and the change of strain with time was recorded.

Optical microscopy(OM). The ESO 0.8 films processed at different die temperatures were observed by an optical microscope (OM, Olympus BX51A, Japan).

Differential Scanning Calorimetry (DSC). Thermal analyses were performed using DSC (Q20, TA, USA). The sample was held at 200 ˚C for 3 min to eliminate thermal history, then cooled to 0 °C at 10 °C/min, and finally heated to 200 ˚C at 10 ˚C/min.

Table S1. Extrusion and film-blowing processing parameters for neat PLA and ESO 0.8.

Samples	Feeding Zone (˚C)	Melting Zone (˚C)	Metering Zone (˚C)	Die (˚C)	The blown bubble
neat PLA-175	150	180	180	175	unstable and uneven
ESO 0.8-175	150	180	180	175	hard to inflate
ESO 0.8-185	160	190	190	185	stable and uniform
ESO 0.8-190	165	195	195	190	stable and uniform
ESO 0.8-195	170	200	200	195	stable and uniform

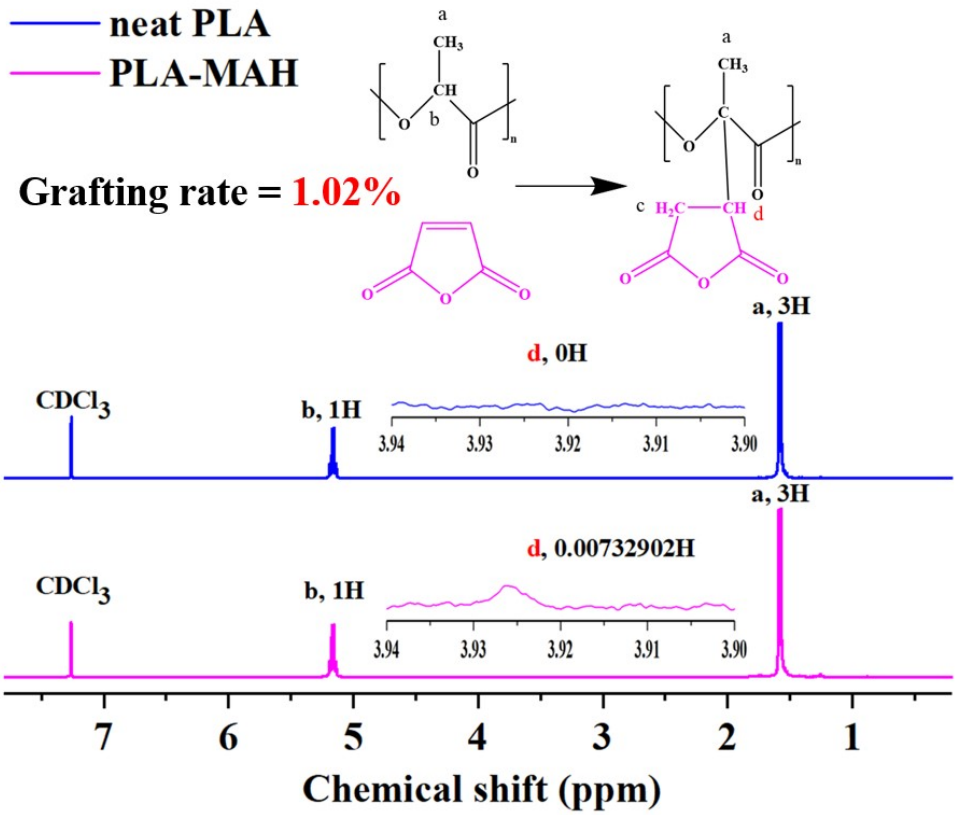

Figure S1. ^{1}H NMR spectra of neat PLA and PLA-g-MA samples. Before testing, the PLA-g-MA samples were soaked in $CDCl_3$ for 24 h to purify the samples. The graft ratio PLA-g-MA is calculated to be 1.02%.

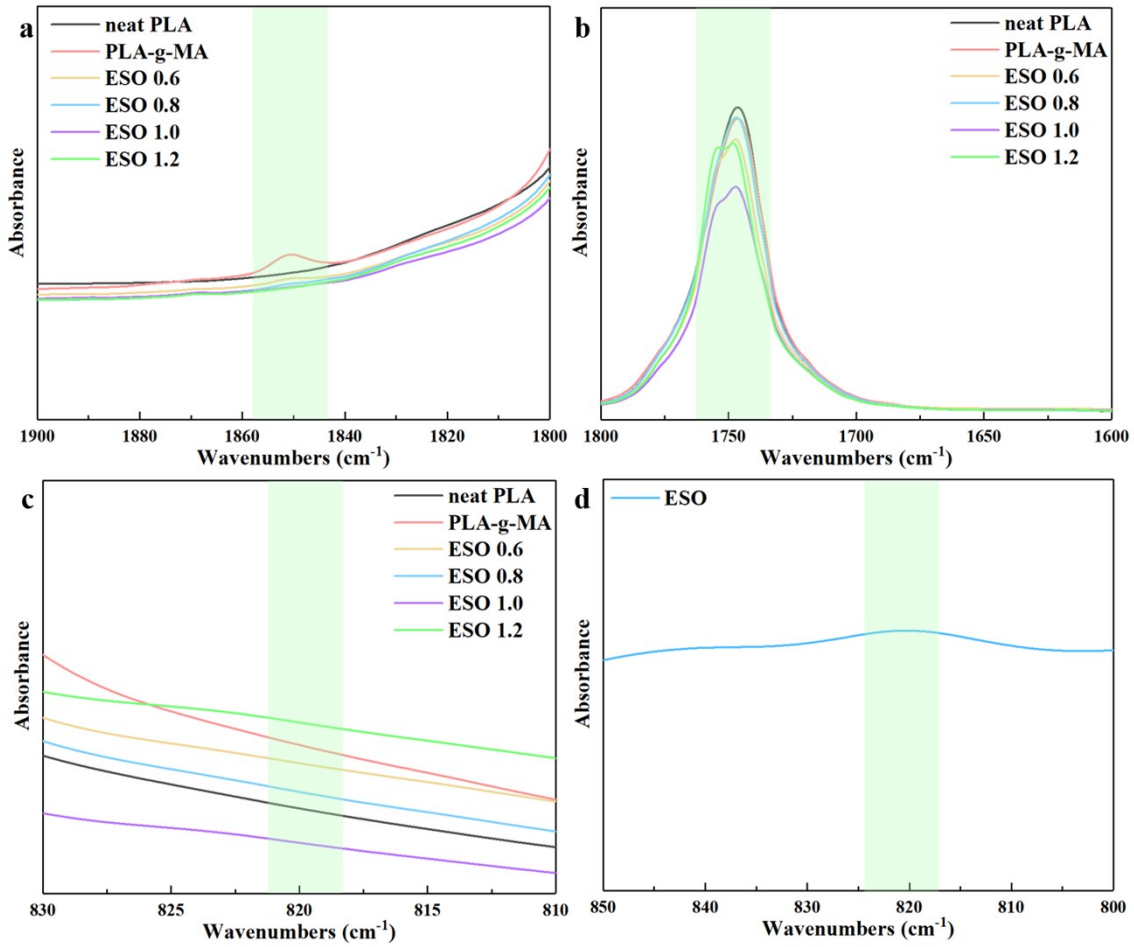

Figure S2. FTIR spectra of neat PLA, PLA-g-MA and PLA CANs at wavenumber range of (a) 1900-1800 cm^{-1}, (b) 1900-1800 cm^{-1}, and (c) 830-810 cm^{-1}. (d) FTIR spectra of ESO at wavenumber range of 850-800 cm^{-1}.

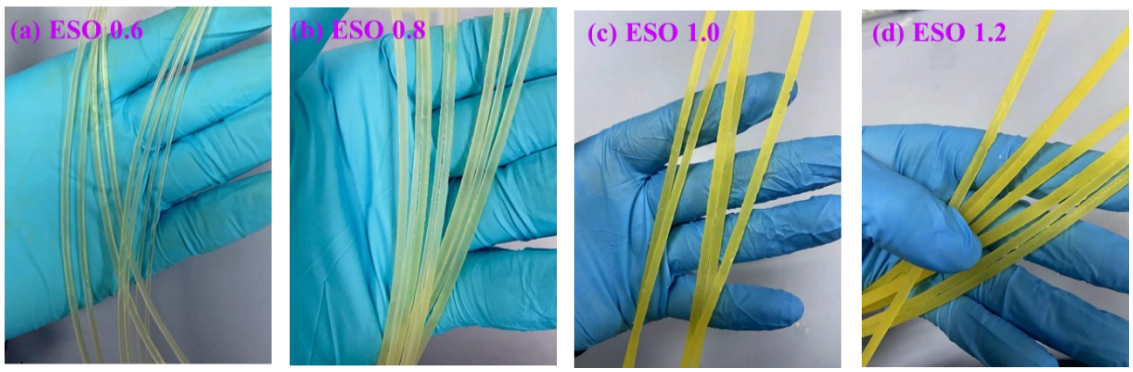

Figure S3. Photographs of extruded samples of (a) ESO 0.6, (b) ESO 0.8, (c) ESO 1.0, and (d) ESO 1.2.

Table S2. The temperature at which the mass loss of 5% ($T_{95\%}$) for all samples.

Samples	neat PLA	ESO 0.6	ESO 0.8	ESO 1	ESO 1.2	PLA /$Zn(acac)_2$	PLA /$Zn(acac)_2$ /ESO	PLA-g-MA	PLA-g-MA /$Zn(acac)_2$
$T_{95\%}$(°C)	338.8	284.2	288.8	285.7	286.2	242.0	210.2	332.2	285.0

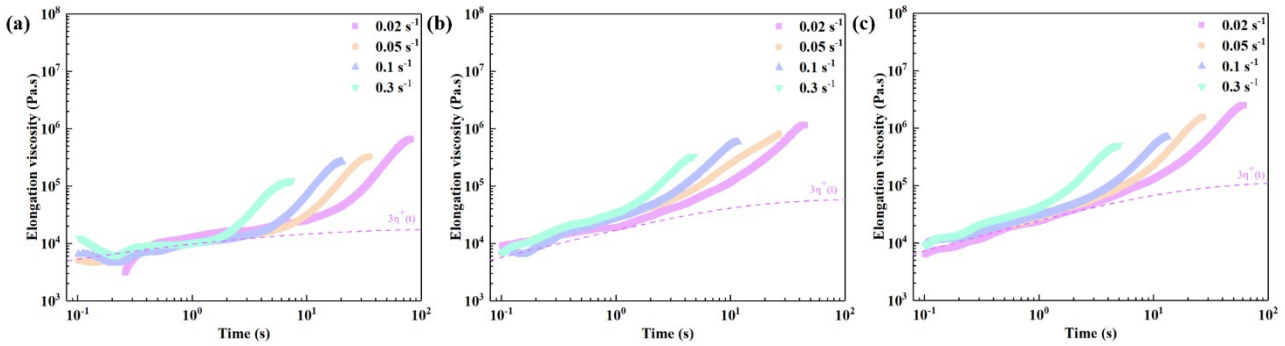

Figure S4. Transient elongational viscosity versus time curves of (a) ESO 0.6, (b) ESO 1.0, and (c) ESO 1.2 at 180 °C and different Hencky strain rates.

Figure S5. Photograph of neat PLA under the melt extensional rheology testing conditions. Neat PLA cannot be tested due to its lower melt strength and lower sag resistance, and it will drip before testing.

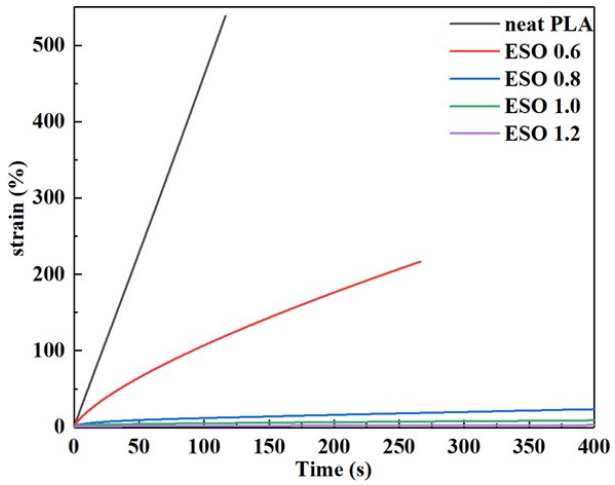

Figure S6. Creep curves of neat PLA and PLA CANs at 185 ˚C.

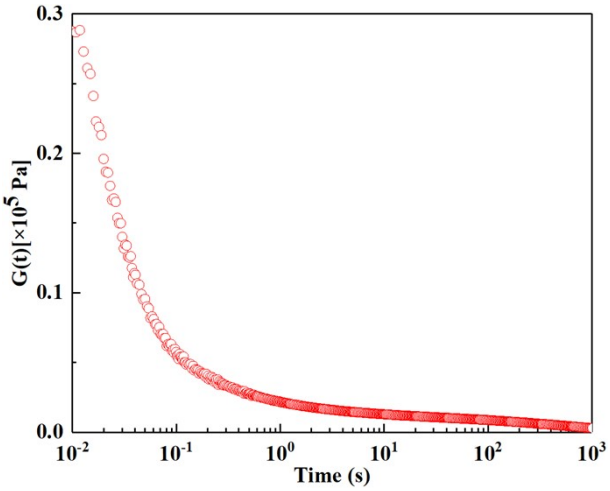

Figure S7. Unnormalized stress relaxation curve of ESO 0.8 at 190 ˚C.

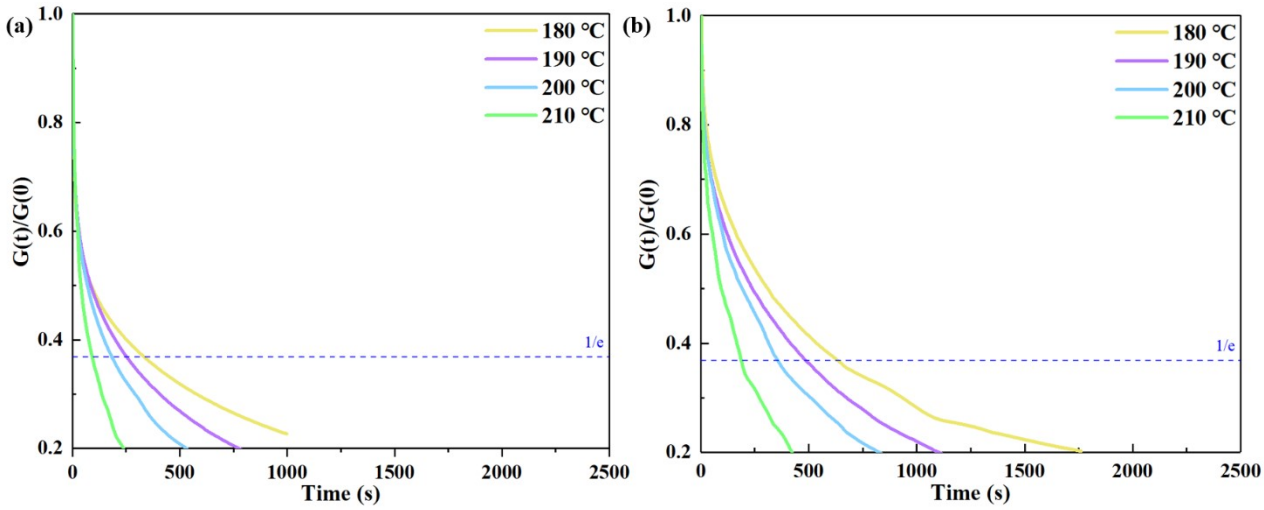

Figure S8. Normalized stress relaxation curves of (a) ESO 0.8 and (b) ESO 1.0 at different temperatures.

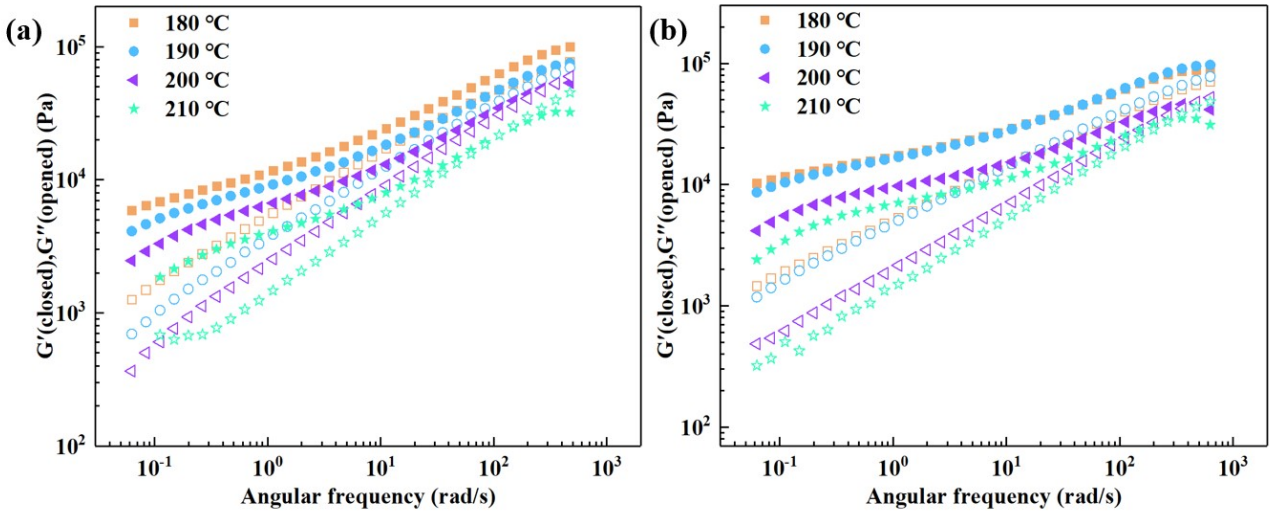

Figure S9. Storage modulus (G′) (closed) and loss modulus (G″) (opened) of (a) ESO 1.0 and (b) ESO 1.2 as a function of angular frequency at different temperatures.

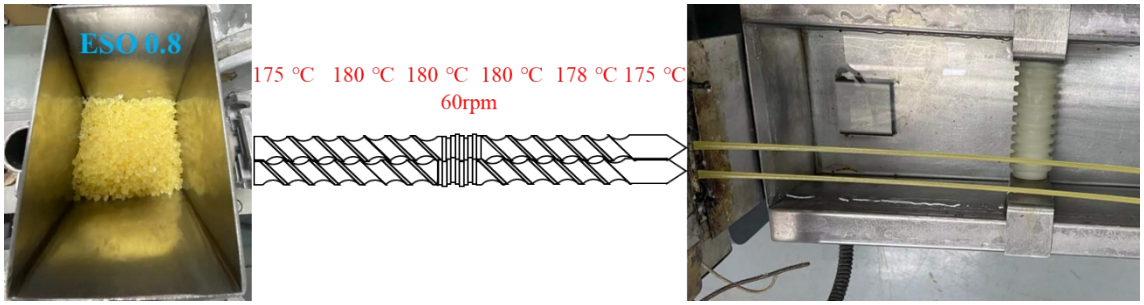

Figure S10. Photographs of ESO 0.8 sample repeatedly processed through a twin screw extruder using the same conditions as those conducted in crosslinking reactive processing.

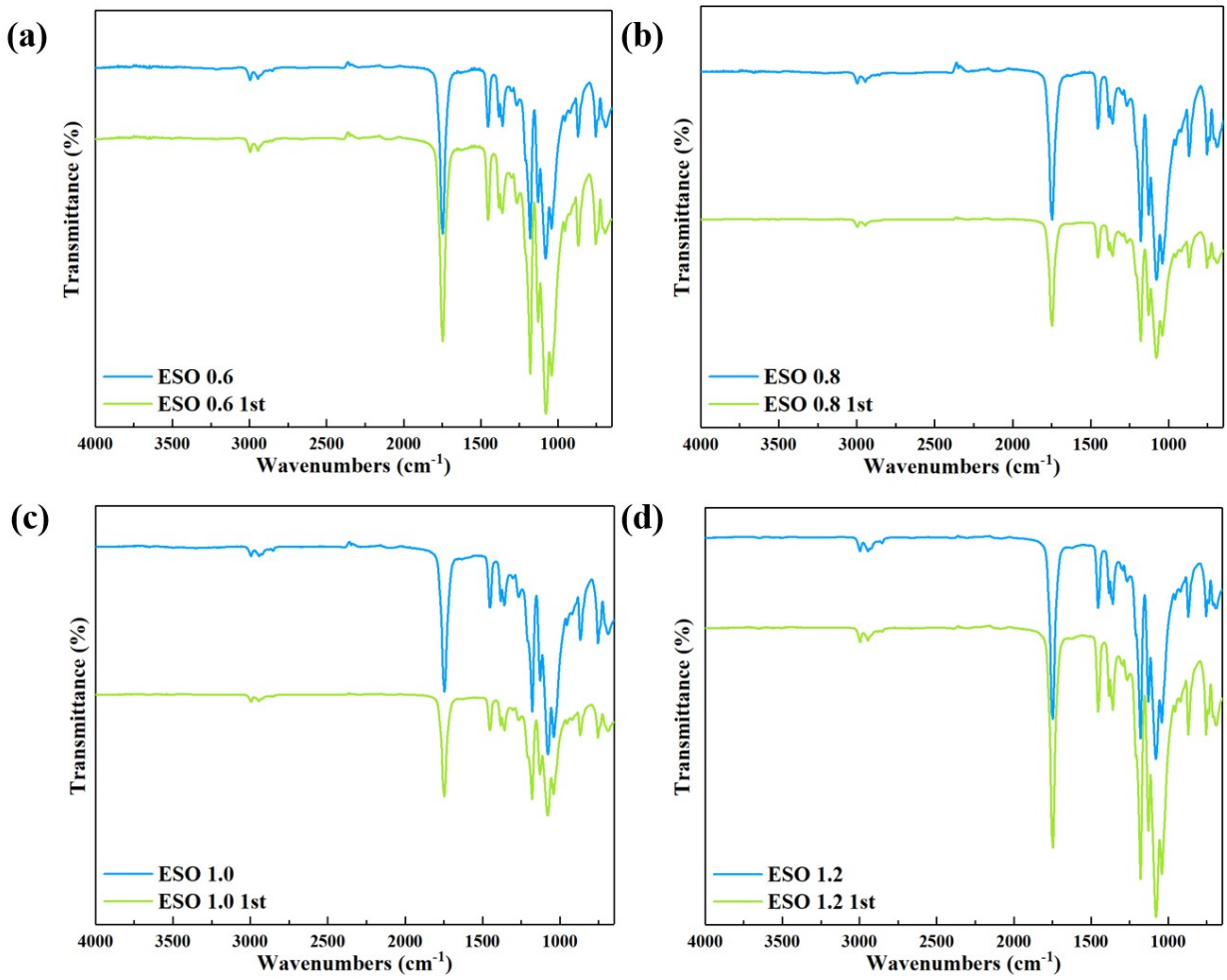

Figure S11. FTIR spectra of original and recycled (a)ESO 0.6, (b)ESO 0.8, (c) ESO 1.0, and (d) ESO 1.2 samples.

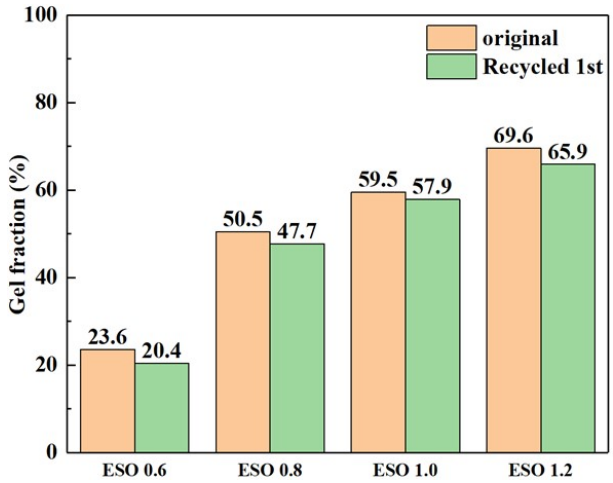

Figure S12. Gel fraction of original and recycled PLA CANs.

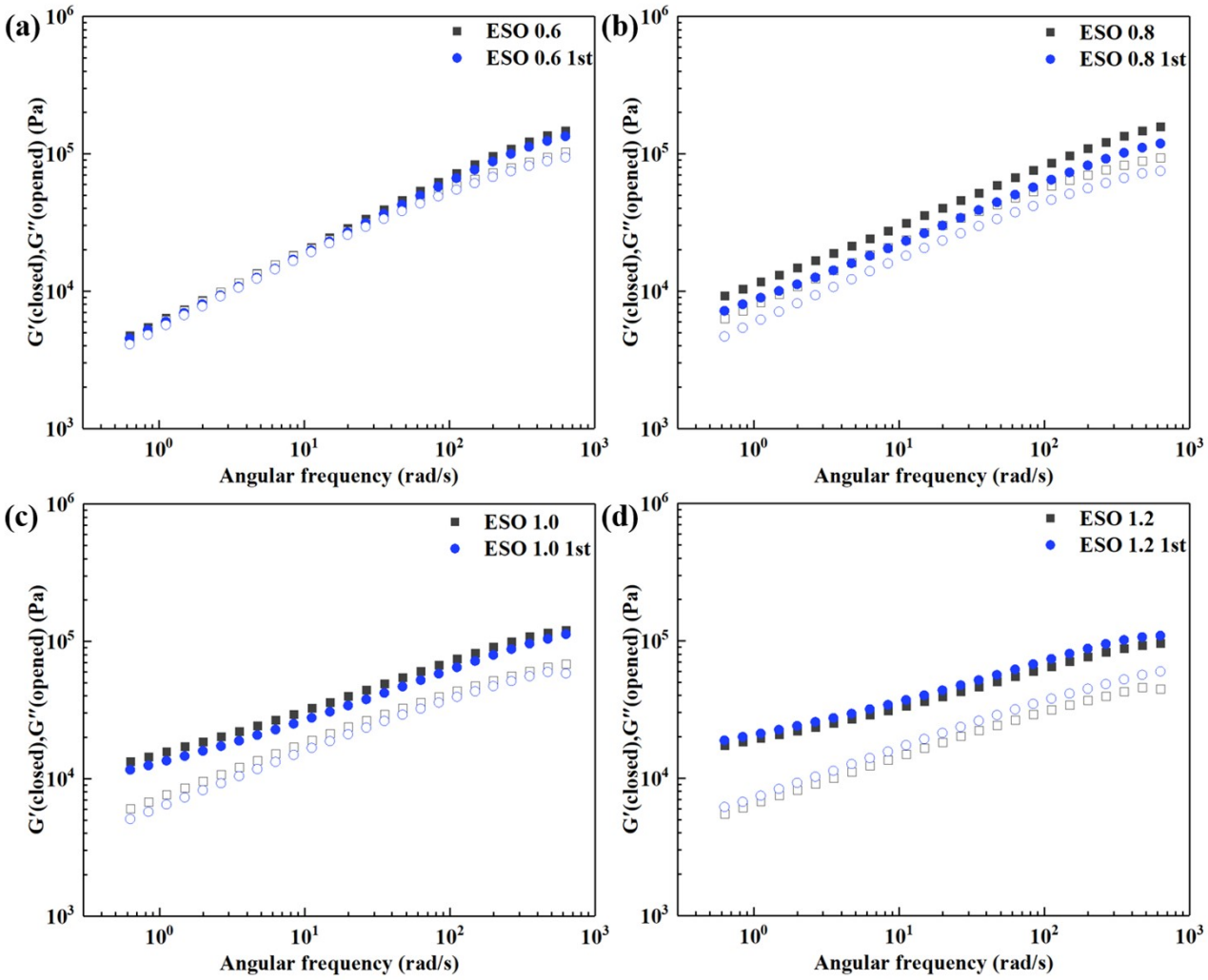

Figure S13. Frequency sweep test of original and recycled (a) ESO 0.6, (b) ESO 0.8, (c) ESO 1.0, and (d) ESO 1.2 samples at 170 ˚C.

Figure S14. Photograph of the film-blowing process of ESO 0.8-175.

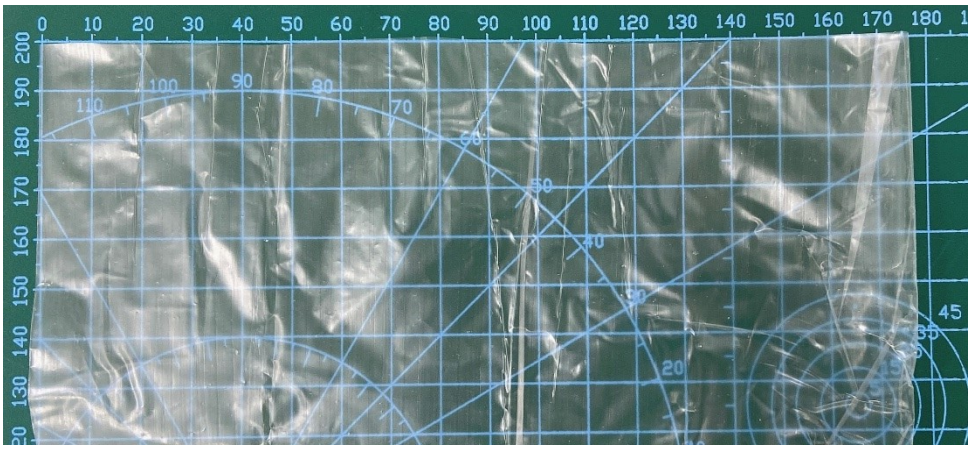

Figure S15. Photograph of ESO 0.8-185 film. (The blow-up ratio is defined as the ratio of bubble diameter to die diameter, and the die diameter is 3 cm)

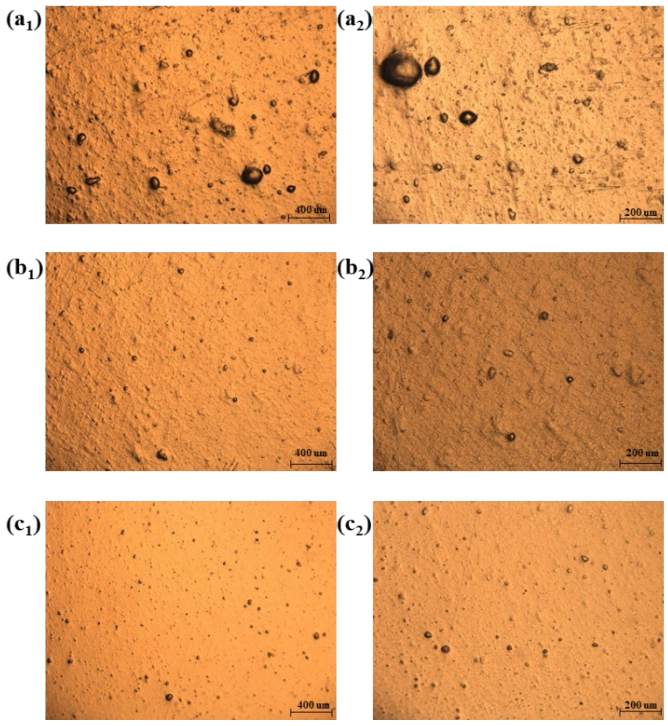

Figure S16. Photographs of ESO 0.8 films processed at different die temperatures observed by an optical microscope: (a_1-a_2) ESO 0.8-185, (b_1-b_2) ESO 0.8-190, and (c_1-c_2) ESO 0.8-195.

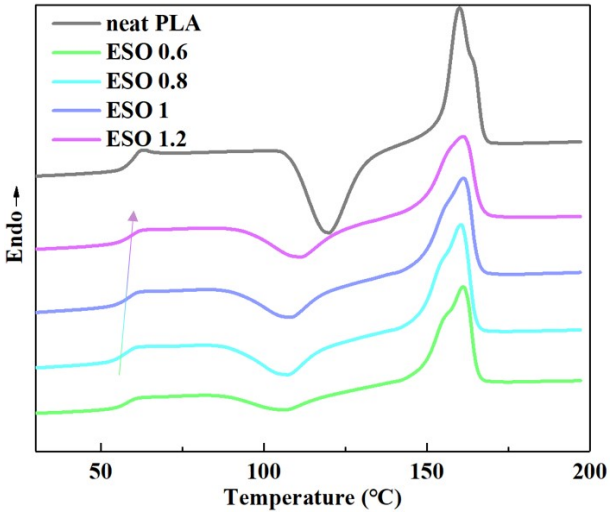

Figure S17. DSC heating curves of neat PLA and PLA CANs after cooling at 10 ˚C/min.

Table S3. Glass transition temperature (T_g) of neat PLA and PLA CANs obtained by DSC measurements.

Samples	neat PLA	ESO 0.6	ESO 0.8	ESO 1.0	ESO 1.2
T_g (˚C)	60.3	58.2	58.1	59.1	59.8

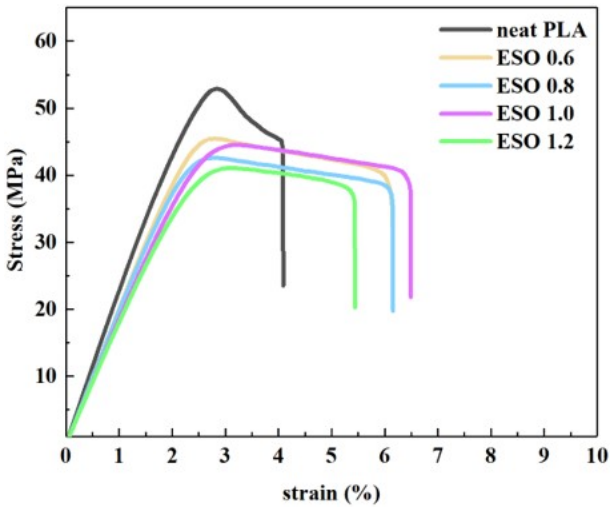

Figure S18. Stress-strain curves of the bulk neat PLA and PLA CANs with a thickness of 0.7 mm prepared by compression molding at 180 ˚C.

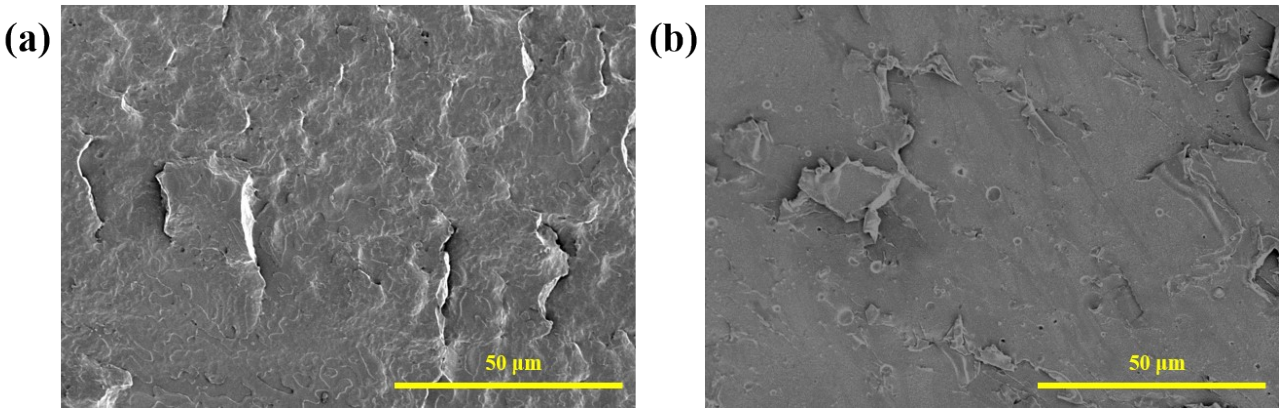

Figure S19. SEM images of the cross-sections of (a) ESO 0.8 and (b) PLA-g-MA/ESO samples prepared by compression molding. PLA-g-MA/ESO was prepared by a torque rheometer (XSS-300, Shanghai Kechuang Rubber Plastics Machinery Set Ltd, China) at 180 ˚C by the following procedure: completely dried PLA-g-MA was first melted at 20 rpm for 3 min, followed by the addition 6.42 wt% ESO and mixed at 60 rpm for 5 min.

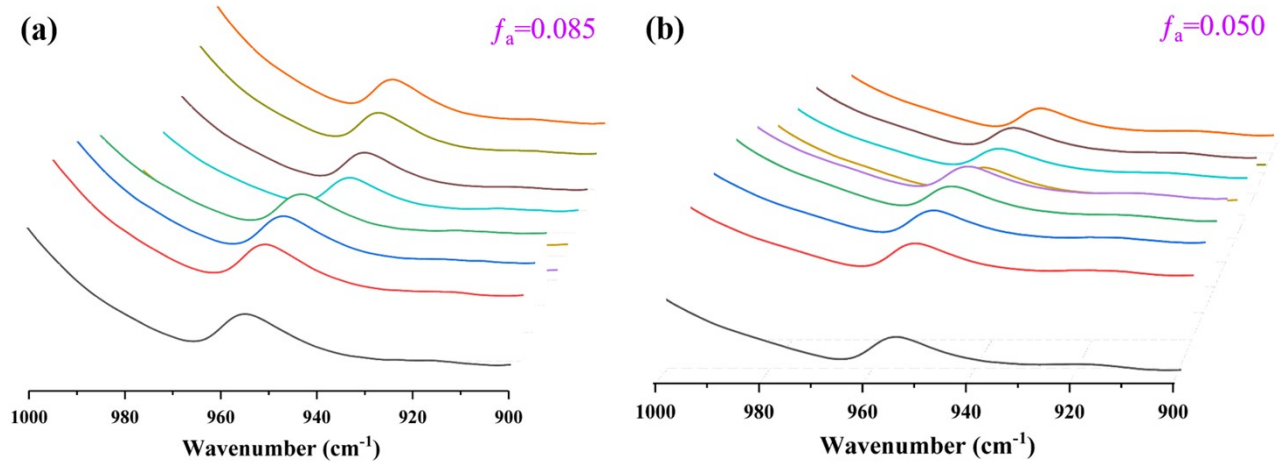

Figure S20. P-FTIR spectroscopy of (a) neat PLA-175 and (b) ESO 0.8-185 films. The orientation factors of 956 cm^{-1} (f_a) are labeled on the pictures.

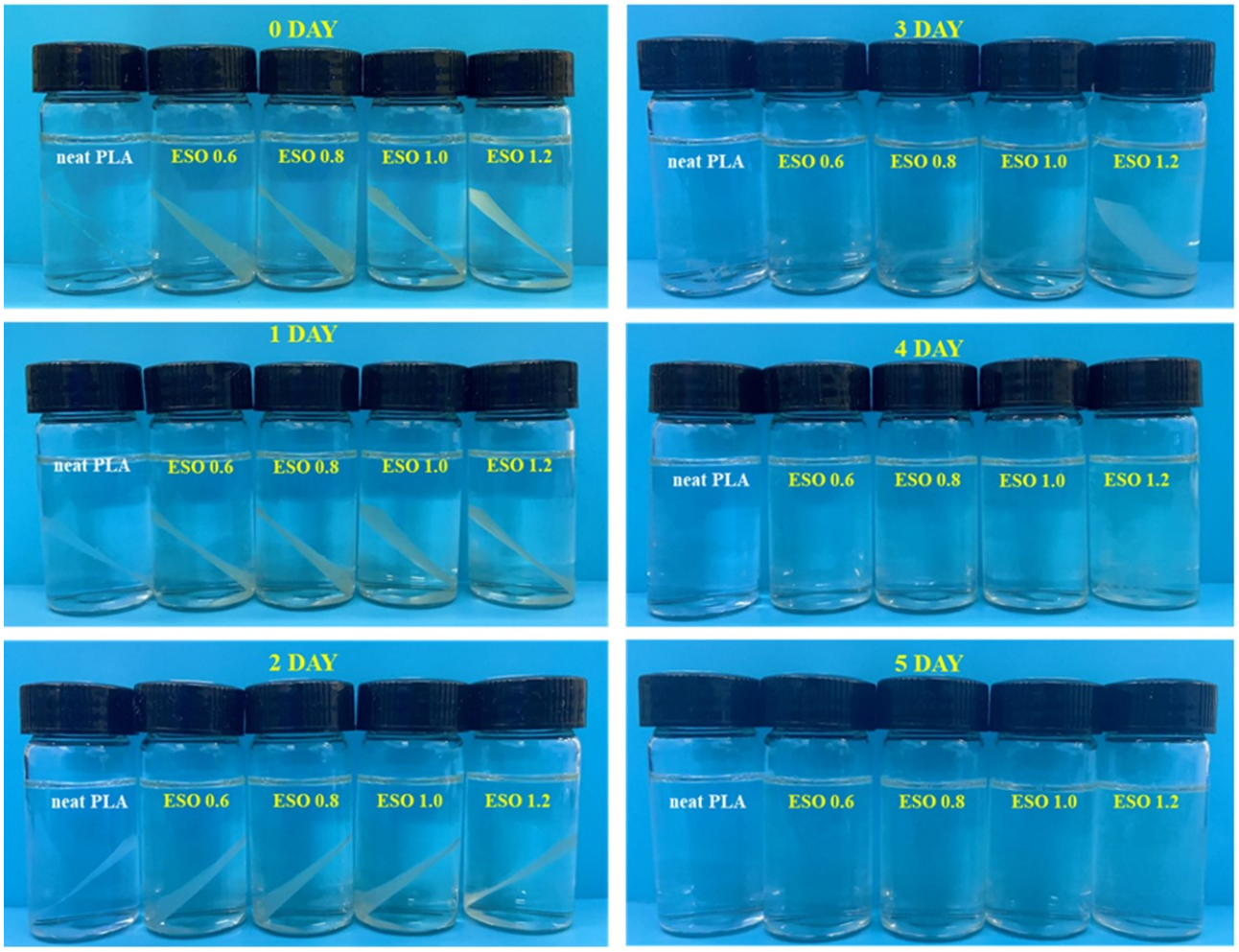

Figure S21. Photographs of neat PLA and PLA CANs degradated for different time in alkaline solution.

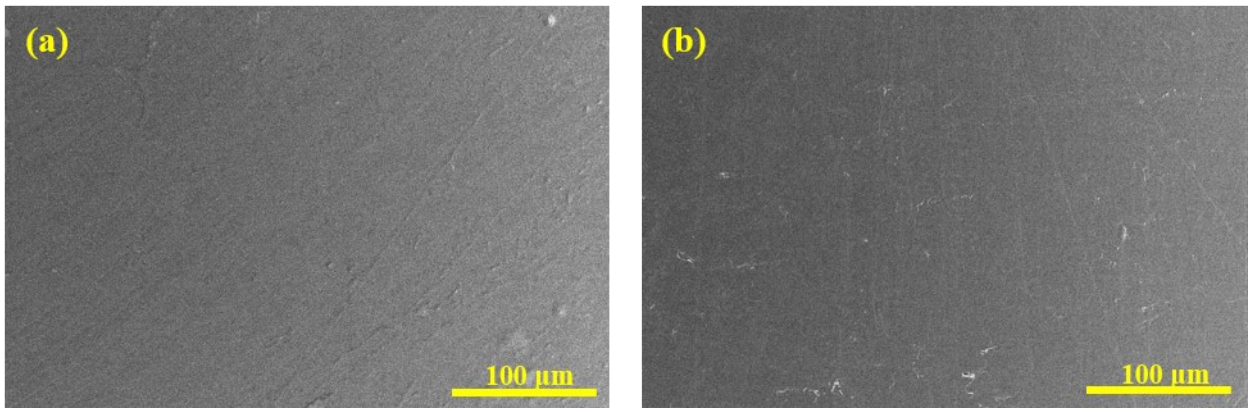

Figure S22. SEM images of the surface of (a) neat PLA and (b) ESO 0.8 before soaking in an alkaline solution.

The specific process of life cycle assessment (LCA).

The LCA analysis was conducted by Simapro 9.0 based on ISO 14040. A functional unit is defined as a plastic film with a mass of 1 kg. The system boundary mainly includes three stages: raw materials, pellet manufacture, and film extrusion. Among them, to simplify the evaluation process, additives whose mass fraction is less than 1%, such as initiator used for PLA CANs preparation, are not considered. The specific process is shown in Figure S23.

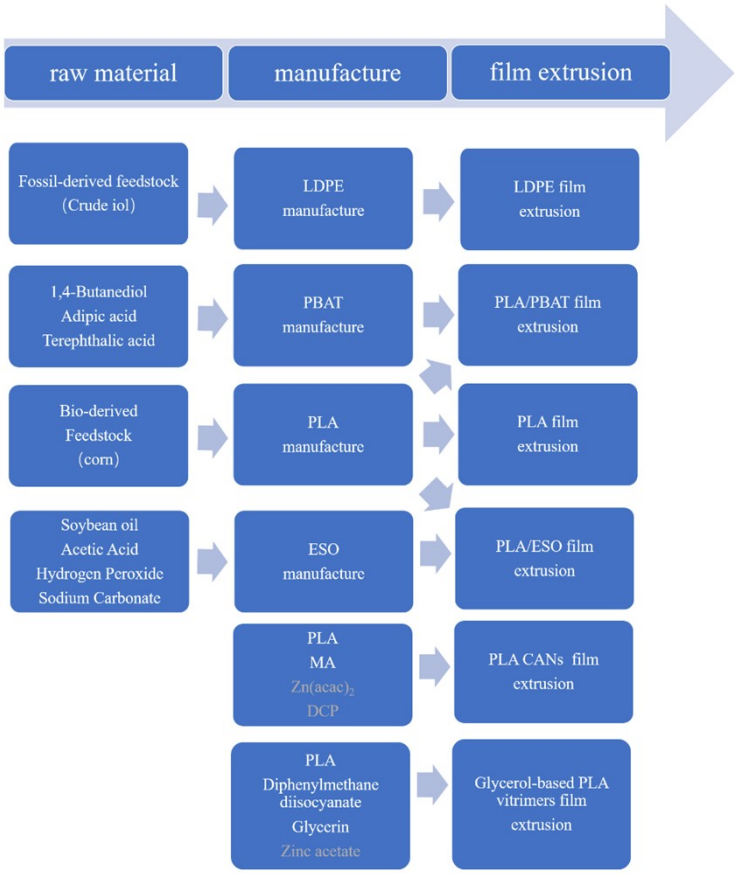

Figure S23. The system boundary of this study.

Table S4. Global warming potential (GWP) of PLA, PLA/PBAT, Glycerol-based PLA CANs, LDPE, PLA/ESO, and PLA CANs films.

Sample	PLA	PLA/PBAT	Glycerol-based PLA CANs	LDPE	PLA/ESO	PLA CANs in this work	
	pellets manufacture						film extrusion
CO_2 eq emissions (kg/kg)	0.62	4.63	1.24	2.01	1.07	0.86	0.57

The data sources of all samples are as follows: The global warming potential (GWP) of PLA is derived from literature reports, and CO_2 equivalent to the production of 1 kg of neat PLA is 0.62 kg[5]. Maleic anhydride, glycerol, diphenylmethane diisocyanate, LDPE, and extrusion data are from Ecoinvent 3.0 database, which can be obtained through simapro software. In the case of PBAT and

ESO, there is no specific data from the environmental databases of Ecoinvent. According to reports in the literature,[6] assuming that the synthesis efficiency of PBAT is 90%, the raw materials required for 1 kg of PBAT are 0.41 kg of 1,4-butanediol, 0.37 kg of adipic acid, and 0.33 kg of terephthalic acid. In addition, its esterification process is comparable to that of polyethylene terephthalate (PET). And the consumption of raw materials to manufacture 1 kg of ESO is as follows: 0.982 kg of soybean oil, 0.117 kg of hydrogen peroxide, 0.196 kg of acetic acid, 0.04 kg of sodium carbonate, 45 kg of water, 0.3 kg of steam and 0.1 KW·h power consumption. On this basis, the databases of PBAT and ESO were compiled and applied in SimaPro software. For the environmental impact assessment process, the GWP was applied and the characterization model, as developed by the Intergovernmental Panel on Climate Change (IPCC), was selected for the development of characterization factors. Factors are expressed as GWP for a time horizon of 100 years (GWP100), in kg CO_2 equivalent/kg emission. Among them, the CO_2 absorption of ESO is calculated by using the biological material storage method. Since the carbon content of ESO is 0.7021 kg/kg ESO, the net absorption of CO_2 is 0.7021/12*44=2.57 kg/kg ESO. In addition, this study also uses the ReCiPe2016 method to explore the scarcity of fossil resources.

Reference

1. M.-H. Wu, C.-C. Wang and C.-Y. Chen, *Polymer*, 2020, **202**, 122743.
2. Y. Wang, Z. Liu, C. Zhou, Y. Yuan, L. Jiang, B. Wu and J. Lei, *J. Mater. Chem. A*, 2019, **7**, 3577-3582.
3. Y. Li, Z. Yao, Z.-h. Chen, S.-l. Qiu, C. Zeng and K. Cao, *Polymer*, 2015, **70**, 207-214.
4. X.-R. Gao, Y. Li, H.-D. Huang, J.-Z. Xu, L. Xu, X. Ji, G.-J. Zhong and Z.-M. Li, *Macromolecules*, 2019, **52**, 5278-5288.
5. E. T. H. Vink and S. Davies, *Industrial Biotechnology*, 2015, **11**, 167-180.
6. B. Choi, S. Yoo and S.-i. Park, *Sustainability*, 2018, **10**, 2369.